Generation of blobs and holes in the edge of the ASDEX Upgrade tokamak

B Nold[1], G D Conway[2], T Happel[3], H W Müller[2], M Ramisch[1], V Rohde[2], U Stroth[1] and the ASDEX Upgrade Team[2]

1 Institut für Plasmaforschung, Universität Stuttgart, 70569 Stuttgart, Germany
2 Max-Planck-Institut für Plasmaphysik, EURATOM Association, Garching, Germany
3 Laboratio Nacional de Fusión, Asociación EURATOM-CIEMAT, 28040 Madrid, Spain

E-mail: nold@ipf.uni-stuttgart.de

Abstract. The intermittent character of turbulent transport is investigated with Langmuir probes in the scrape-off layer (SOL) and across the separatrix of ASDEX Upgrade Ohmic discharges. Radial profiles of plasma parameters are in reasonable agreement with results from other diagnostics. The probability density functions of ion-saturation current fluctuations exhibit a parabolic relation between skewness and kurtosis. Intermittent *blobs* and *holes* are observed outside and inside the nominal separatrix, respectively. They seem to be born at the edge of the plasma and are not the foothills of avalanches launched in the plasma core. A strong shear flow was observed 1 cm radially outside the location where blobs and holes seem to be generated.

1. Introduction

One of the big challenges on the way to controlled fusion in magnetically confined plasmas is a better understanding of turbulent cross-field transport. On the one hand, radial transport is needed to extract impurities and helium ash out of the plasma core. On the other hand it limits plasma confinement. Especially at the plasma edge and in the scrape-off layer (SOL) turbulent transport is far from being understood. In this region a better understanding is of great importance, since transport defines the width of the edge pedestals of density and temperature and therefore the energy content of the plasma. In the SOL, turbulent transport determines the peak power load onto the divertor plates and radially propagating intermittent structures can lead to a high power flux to the first wall.

Since many years, turbulent transport is investigated in the edge of tokamaks and stellarators by means of Langmuir probes [1–6] and optical diagnostics [7,8] (for a review, see Ref. [9]). Intermittency has been identified as an universal feature of turbulent fluctuations in L-mode [10] and in between ELMs during H-mode plasmas [11]. In the SOL the intermittent events appear as positive density fluctuations and thus have been named blobs. Blobs have been observed not only in toroidally confined plasmas, but also in linear devices without magnetic field curvature [12–14] and in a simple magnetized torus, where all field lines are connected to the wall [15, 16]. While the radial drift of the blobs could be clarified (at least for toroidal devices) to be due to the self-generated $E\times B$ drift caused by the charge separation by curvature drifts [17], the generation of blobs remains blurred. An interchange mechanism active at the separatrix has been concluded from fluid simulations [18–21]. In the basic toroidal experiment TORPEX, without closed field lines, an interchange instability was found to be responsible for blob generation [15,16], while in the linear experiments VINETA and CSDX, the blobs emerge out of quasi-coherent drift waves [13, 14]. In the toroidally confined low-temperature plasma of TJ-K, blobs have been shown to be generated from drift-wave turbulence in the confinement region due to a change of turbulent characteristics across the separatrix [22]. Using a fast camera on the high-temperature plasma of the NSTX tokamak, a blob birth zone was identified in the SOL around the steepest normalized pressure gradient [23].

Hence, although quasi-coherent density fluctuations or blobs are clearly identified to play an important role for transport in the SOL, the instability responsible for blob generation as well as the exact spatial location of their birth have not been identified yet unambiguously. The present work presents results of a study carried out with Langmuir probes in the SOL of the ASDEX Upgrade tokamak. In Ohmically heated discharges it was possible to probe the plasma across the separatrix. The study indicates a birth region of blobs close to the separatrix. An interchange-type of mechanism is consistent with these observations.

The paper is organized as follows: the next section gives information on the experimental setup and the discharges investigated. The experimental results on background profiles, statistical properties of the density fluctuations and on their

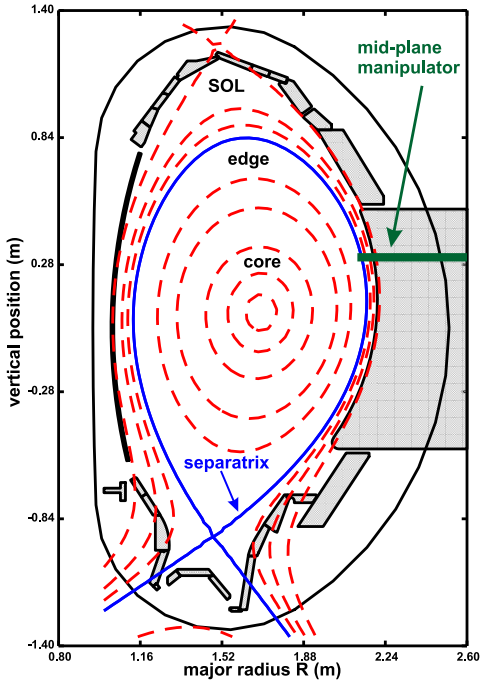

Figure 1. Poloidal cross-section of ASDEX Upgrade, showing the magnetic geometry of a lower single null discharge and the position of the mid-plane manipulator.

poloidal propagation are presented in Secs. 3, 4 and 5, respectively. A summary and discussion are given in Sec. 6.

2. Experimental setup

Langmuir probe measurements were carried out in the SOL of the divertor tokamak ASDEX Upgrade [24], which has major and minor radii of $R = 1.65$ m and $a = 0.5$ m, respectively. In order to be able to carry out probe measurements across the separatrix, the investigation was focused on Ohmically heated discharges. The deuterium discharges were realized in the magnetic lower single null configuration, as shown in figure 1. The plasma current was $I_p = 800\,\mathrm{kA}$, the toroidal magnetic field strength $B = 2\,\mathrm{T}$ (clockwise), the edge safety factor $q_{95} \approx 4$ and the line averaged density $\overline{n} \approx 4.2 \times 10^{19}\,\mathrm{m}^{-3}$. In the separatrix region, the drift scale length $\rho_s = c_s/\omega_{ci}$ was about 0.4 mm, with the ion sound velocity $c_s = \sqrt{T_e/m_i} \approx 38\,\mathrm{km/s}$ and the ion gyro frequency $\omega_{ci} = eB/m_i \approx 9.6 \times 10^7\,\mathrm{s}^{-1}$. The electron-diamagnetic drift velocity $\mathbf{u}_{dia,e} = \nabla p_e \times \mathbf{B}/enB^2$ was about 3 km/s at the separatrix and upward directed at the low-field side of the torus.

The Langmuir probes were fixed on a solid carbon probe head mounted on the reciprocating mid-plane manipulator. The manipulator penetrates the plasma horizontally from the low-field side about 30 cm above the outer mid-plane (see figure 1) with a speed of about 1 m/s. Figure 2 shows the probe head as seen from the plasma side. 14 probe tips are embedded on three different levels in a carbon block. The

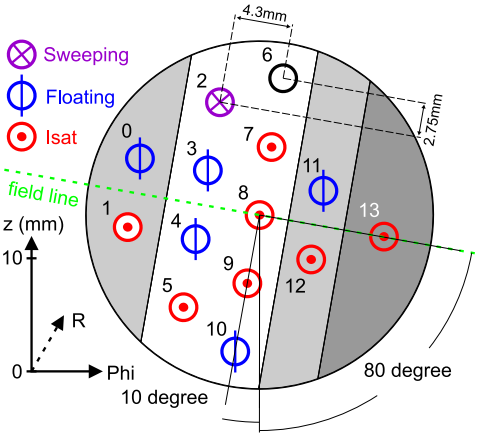

Figure 2. Sketch of the probe head as seen from the plasma side. The symbols indicate whether a tip was connected to measure ion-saturation current, floating potential or the entire Langmuir probe characteristics.

cylindrical carbon tips have a radius of 0.45 mm and a length of 2 mm. These small free standing probe tips minimize the perturbation of the plasma by the probe, but may easily burn if the power load exceeds a certain limit. The dashed line in figure 2 indicates the inclination of the magnetic field lines in front of the manipulator for an edge safety factor of $q_{95} \approx 4$. The probe head is tilted by 10° such that the probe tips on the front level (white background in figure 2) form an array perpendicular to the magnetic field lines with a distance of 2.75 mm between neighboring tips. The tips on the gray background are retracted by 4 mm and tip number 13 is retracted by 8 mm with respect to the front level tips (white background). The different symbols in the figure indicate which of the tips were connected to measure ion-saturation current or floating potential. Tip number 2 was used to measure the full current-voltage characteristics, which were analyzed to obtain electron temperature profiles. The tips measuring ion-saturation current were biased to −180 V with respect to the vacuum vessel to assure that electrons are rejected even at negative plasma potential and high temperature close to the separatrix. Probe current and voltage signals were recorded with an acquisition rate of 2 MHz.

In each discharge, two strokes have been carried out at different density levels. The ion-saturation current fluctuation data presented in this article was taken from probe tips 8 and 9 during the second stroke in discharge #24111 and is representative for these discharge parameters. In some measurements, a hysteresis was observed between signals recorded during inward and outward motion of the probes. This might be attributed to a high heat load on the probe tips at the innermost position, causing electron emission and arcs. The data presented in this work were mainly recorded during the inward motion of the manipulator, when the tips were still cold. During this phase, the probes provide fluctuation data for about 1 ms/mm. Hence, there are 2000 data points on a millimeter which is rather little for statistical analysis. However, the validity of the results was checked for consistency by comparing data from different probe tips in several

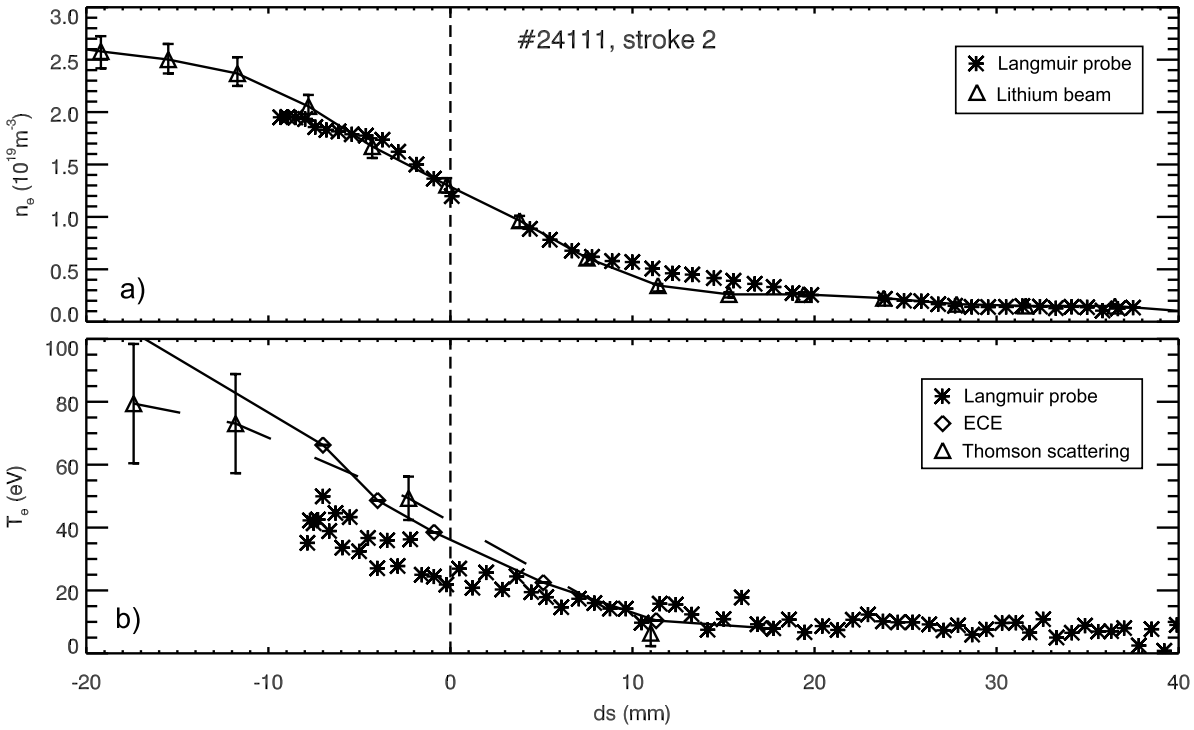

Figure 3. Equilibrium profiles in the boundary of ASDEX Upgrade tokamak during Ohmic discharge #24111. a) Plasma density from lithium-beam diagnostic (△) and deduced from the ion-saturation current corrected (∗). b) Electron temperature from Thomson scattering (△), electron-cyclotron emission (⋄) and Langmuir probe characteristics (∗). d_s is the distance to the nominal separatrix at the magnetic midplane.

discharges.

3. Equilibrium Profiles

Background pressure gradients drive plasma flows and turbulence. Hence, for the interpretation of the fluctuation measurements, a good knowledge of the equilibrium profiles is crucial. Figure 3 shows profiles of the background density n_e and electron temperature T_e as a function of the distance d_s to the nominal separatrix position. This position is obtained from the magnetic field reconstruction with a radial uncertainty of about $\pm 5\,\mathrm{mm}$.

In figure 3a, the electron density profile from the lithium beam diagnostic (LIN) [25, 26] is shown together with the density obtained from probe measurements. The electron density was deduced from the ion-saturation current measured with probe tip number 9, taking into account the factor $\sqrt{T_e}$ and an effective probe surface of $5\,\mathrm{mm}^2$. Good agreement is found in the entire range.

Figure 3b compares the electron temperature profiles deduced from the probe characteristics (tip number 2) with results from the electron-cyclotron emission (ECE) radiometer [27] and the Thomson scattering diagnostics [28]. The temperature decreases

from about 50 eV in the confined plasma to $5 - 10$ eV in the far SOL. Good agreement is found in the SOL. Close to the separatrix and in the confined plasma, the swept Langmuir probe underestimates the electron temperature systematically, which might be due to the temperature and potential fluctuations [29].

The density and temperature profile scale lengths at the separatrix were found to be $L_n = |\nabla \ln n_e|^{-1} \approx 1.2 \pm 0.2$ cm and $L_T = |\nabla \ln T_e|^{-1} \approx 1.1 \pm 0.4$ cm, respectively. In the discharge investigated here, the values of the two perpendicular scale lengths were of the same order, which is not common for ASDEX Upgrade discharges (typically $L_n \approx 2 \times L_T$) but possible in Ohmic discharges.

The diagnostics exploited for this work measure at different toroidal and poloidal positions in the torus and had to be mapped along the reconstructed magnetic field to the outer magnetic midplane. Radial shifts (Thomson +5 mm, lithium beam and probes −5 mm, ECE +3 mm) have been applied to account for a toroidal asymmetry in the distance between vacuum vessel and magnetic field geometry, which is not captured by the field reconstruction.

4. Statistic properties of the fluctuations

In the following, the results of statistical analyses of fluctuations in the ion-saturation current are presented. The data were measured with tip number 9 during the inward motion of the probe in shot #24111. Analysis are mostly based on time windows of 1024 μs containing 2048 data points. During this time the probes advance by 1 mm. Taking into account the length of the probe tip, the radial uncertainty is ± 1.5 mm. The time windows of two neighboring radial positions have an overlap of 1024 time points, this means that every measurement is considered twice, to increase the radial resolution.

Figures 4a-c show three sub windows of the raw signal corresponding to characteristic radial positions around the separatrix from $d_s = -4$ to 5 mm. The large spikes with amplitudes in excess of 2 standard deviations are a first signature of intermittency, as it was observed in many other devices, too [10, 30, 31]. The spikes are mostly negative in the confined plasma ($d_s = -4$ mm) and mostly positive in the SOL at $d_s = 5$ mm. At the nominal separatrix ($d_s = -1$ mm), they are almost equally distributed. The skewness of the probability density function (PDF) is a measure of this asymmetry, as can be seen by comparing the PDFs to a Gaussian with the same standard deviation (Figs. 4d-f). The skewness value shown in the figures is given by $S = \langle (x - \langle x \rangle)^3 \rangle / \langle (x - \langle x \rangle)^2 \rangle^{3/2}$. At the separatrix, positive and negative density fluctuation amplitudes are equally distributed and the PDF is well represented by a Gaussian (Figs. 4b,e). Consequently, the skewness at this position is close to zero. In the confined plasma, the PDF exhibits a wing at large negative amplitudes and a lack of such events on the positive side, leading to a negative skewness of −0.63 (Figs. 4a,d) whereas in the SOL the situation is reversed and the skewness is positive with +0.87 (Figs. 4c,f). This change of sign as well as the position where it happens are in remarkable agreement with earlier findings from DIII-D [6]. It is interesting to

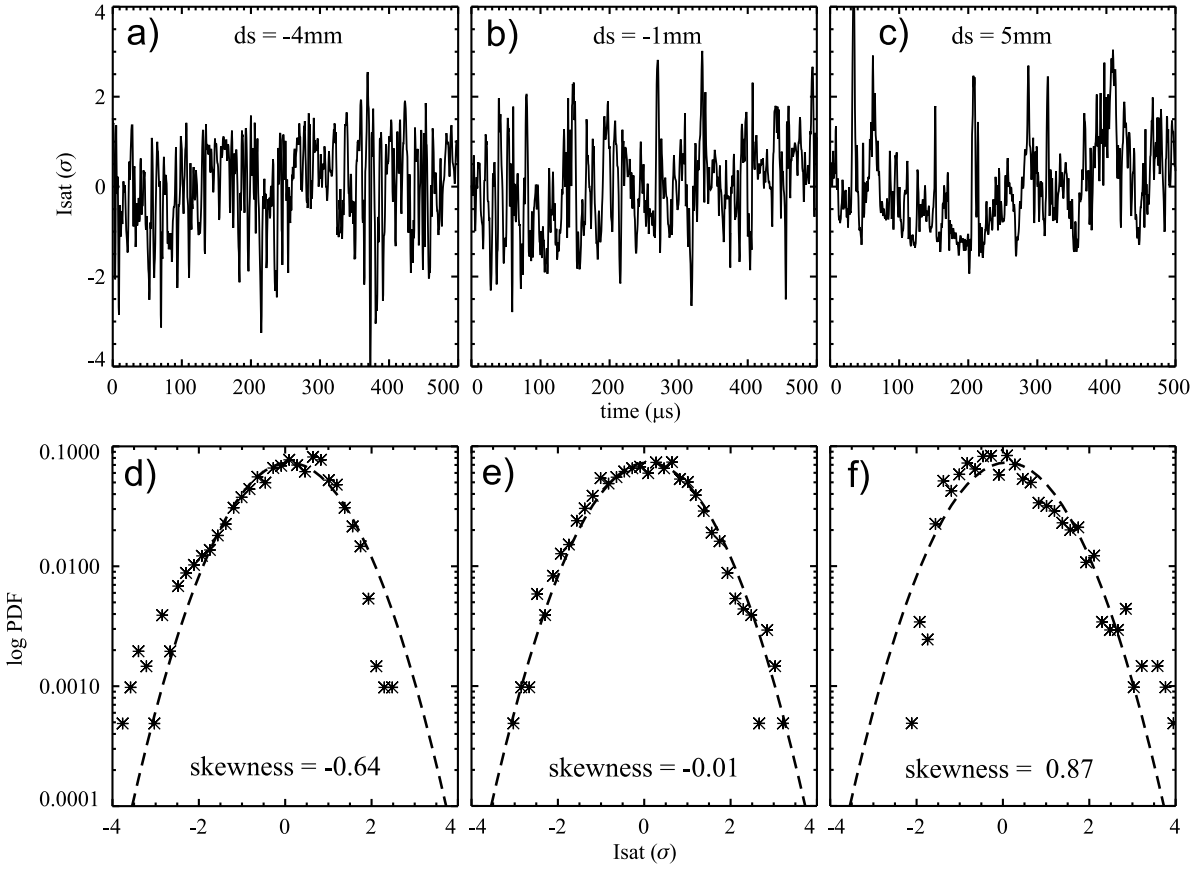

Figure 4. Ion-saturation current fluctuations around the separatrix, normalized to their standard deviations (top) and the corresponding probability density functions (bottom).

note, that investigations of the skewness profiles on the limiter tokamak TEXTOR [32] and of limited discharges in JET [33] did not show a zero transition of the skewness at all or further inside the confined plasma, respectively.

Figure 5 depicts radial profiles from $d_s = -10$ to $+40$ mm of statistical moments calculated from the ion-saturation current fluctuations. The gaps in the ranges $d_s = 0$ – 4 mm, 20 – 24 mm and 38 – 40 mm result from the bias voltage being switched off in order to extinct possible arcs between probe head and pins. The fluctuation amplitude normalized to the mean value is shown in figure 5a. The amplitude slightly decreases from 15 % at the innermost position to about 10 % at $d_s = -5$ mm. Around the separatrix, the relative amplitude increases rapidly and reaches about 40 % at $d_s \approx +7$ mm. Further outside in the SOL, the normalized amplitude remains roughly constant. The inner two centimeters shown here coincide with the region of steepest density gradient (see Fig. 3a), while the highest fluctuation level is found radially further outside. The radial dependence of the skewness is shown in figure 5b. The skewness assumes negative values just inside the separatrix with a minimum at $d_s = -4$ mm, as pointed out earlier in Figs. 4a and 4d. Close to the separatrix, the skewness assumes small values as expected from the fact that positive and negative amplitudes are equally

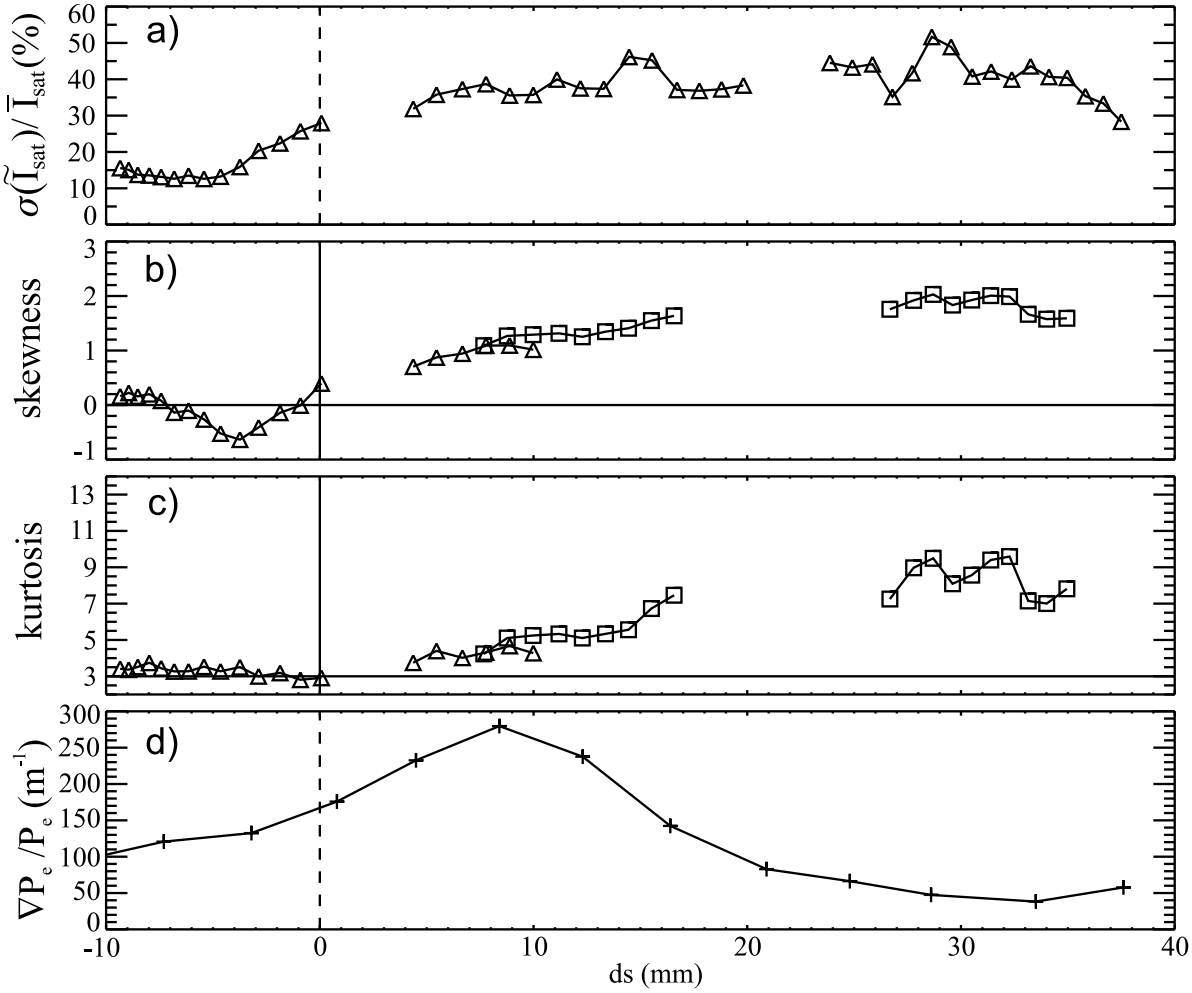

Figure 5. Radial profiles of the statistical moments from ion-saturation current fluctuations and the normalized electron pressure gradient in the edge/SOL region of ASDEX Upgrade.

distributed as it was already shown in Figs. 4b and 4e. The skewness increases across the separatrix until it reaches a value of about 1 at $d_s \approx 7\,\mathrm{mm}$, pointing to the dominance of large positive events (see also Figs. 4c and 4f). Further outside in the SOL, the skewness is positive throughout with values larger than 1. The triangles represent statistics based on 1 ms of fluctuation data, while the squares were calculated using 4 ms time traces to assure convergence.

The kurtosis or peakedness is defined as $K = \langle (x - \langle x \rangle)^4 \rangle / \langle (x - \langle x \rangle)^2 \rangle^2$. Figure 5c shows a profile of the peakedness from ion-saturation current fluctuations. In the confined plasma it is almost constant at the Gaussian value of 3. In the near SOL it increases to about 5, indicating a more peaked PDF. For $d_s > 15\,\mathrm{mm}$, the kurtosis increases further to values around 8. The high kurtosis values indicate that the fluctuations become more intermittent at larger distances from the confined plasma.

In recent literature, positive and negative intermittent events in the edge/SOL region have been addressed as blobs and holes, respectively [6, 12]. The observations

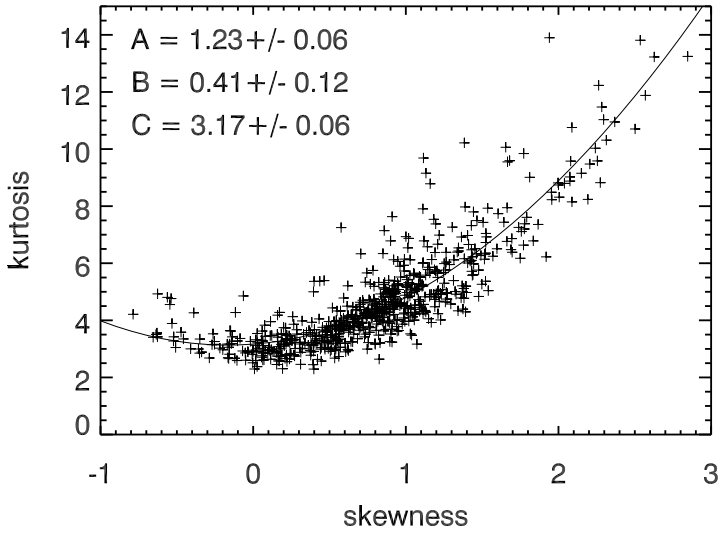

Figure 6. Dependence of the fourth order moment (kurtosis) on the third order moment (skewness) of the PDF of ion-saturation-current fluctuations during an entire stroke in the ASDEX Upgrade discharge #24111.

from above agree with this picture of blobs and holes as isolated positive and negative density structures propagating radially outward and inward, respectively. Radially propagating blobs basically transport plasma from regions of higher density to regions of lower density. If such blobs travel in a steep density gradient, they cause an increasing fluctuation level, as it is observed around the separatrix.

The fact that blobs and holes are spatially separated – in the PDFs in Figs. 4d, f one sees large scale non-Gaussian contributions always only on one side of the PDFs and not on the other – points to a joint generation of them in a narrow layer in-between. Blobs propagate radially outwards to the wall as reported in Refs. [17, 32–35], while the holes decay further inside after a few millimeters in the turbulent environment of the edge plasma. The blobs observed in the SOL cannot originate from far inside the confined plasma, since there is no indication of positive wings in the PDF at $d_s = -4\,\mathrm{mm}$. Hence, the picture can be discarded that blobs are foothills of avalanches launched in the plasma core. The birth region can be identified with the separatrix, were the skewness crosses the baseline. The generation of blobs and holes in this region is also indicated by the radially increasing relative fluctuation level in figure 5a.

Figure 5d shows the normalized electron pressure gradient $\nabla p_e/p_e$ calculated from from ECE and lithium beam data. The peak of this profile indicates the region of maximum linear growth-rate for pressure gradient driven plasma instabilities. Large fluctuation amplitudes can occur in this region, which is close to the blob birth region as identified above. This is consistent with results from the NSTX tokamak, where the birth region was localized by plasma imaging at the maximum of $\nabla p_e/p_e$ in the SOL [23].

To complete the statistical analysis, a recent finding is tested on the present data set. In the basic toroidal plasma experiment TORPEX and the SOL of the tokamak TCV, it was found that skewness S and kurtosis K from the PDFs of ion-saturation current

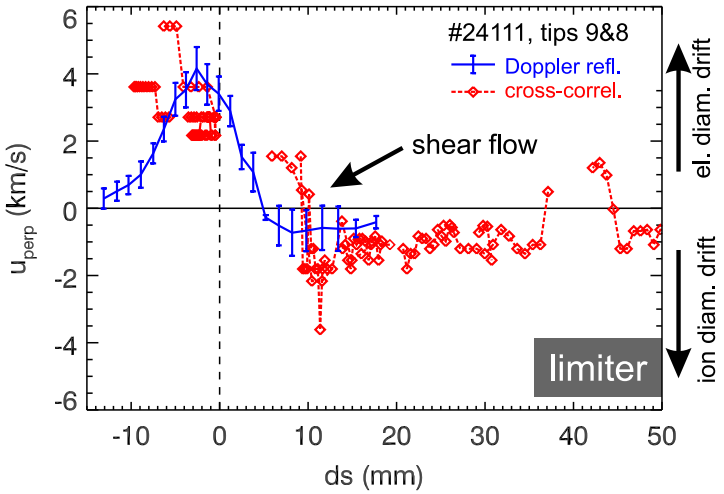

Figure 7. Perpendicular propagation velocity of coherent structures at different distances to the separatrix deduced from Langmuir probe cross-correlation analysis ($\diamond$) and Doppler reflectometry (solid line).

fluctuations follow the parabolic relation $K = aS^2 + bS + c$ with $b = 0$ [36]. Similar results with $b \neq 0$ were also reported from other fusion devices [37]. Figure 6 depicts the dependence of the kurtosis on the skewness from fits to PDFs of ion-saturation current fluctuations of ASDEX Upgrade. Data from the entire stroke analyzed above are included. A quadratic function was fitted to the distribution and its parameters are indicated in the figure. The parabola represents the data rather well, which is consistent with observations made on devices with very different magnetic configurations and plasma parameters.

5. Poloidal propagation

The perpendicular propagation velocity of coherent structures was investigated by cross correlation analysis between the probe tips number 8 and 9 (see figure 2). The velocity $u_\perp = \Delta/\tau$, with the distance between the probes $\Delta = 5.5\,\mathrm{mm}$ and the time delay τ of the correlation maximum. Since the probe array is tilted by 10° with respect to the poloidal direction, the measured velocity is perpendicular to the magnetic field and slightly different from the poloidal velocity. Figure 7 depicts the velocity profile based on data from both inward and outward motion of the probes during the second stroke in discharge #24111. The discrete values showing up at high velocities are imposed by probe distance and sampling rate, whereby the highest detectable velocity (11 km/s for this probe distance) is not yet reached. The probe results agree quantitatively with the perpendicular velocities obtained from Doppler reflectometry (solid line). The latter are based on a profile, which is a tanh fit to the densities from Thomson scattering, lithium beam and laser interferometry to obtain a consistent smooth shape. The radial shifts mentioned in Sec. 3 were applied to the profiles before fitting, to account for the toroidal asymmetry of the torus. As the probes, the Doppler reflectometer is sensitive

to the perpendicular propagation velocity $u_\perp = u_{E\times B} + u_{ph}$ of density perturbations, with the flow velocity $u_{E\times B}$ and the phase velocity u_{ph}. In the present discharge, the reflectometer was set to be sensitive to $k_\perp \approx 7.5 - 10\,\mathrm{cm}^{-1}$, which corresponds to a structure size of about 7 mm. The same structure size is investigated with the probes, as will be shown later. It has been shown that $u_\perp$ is dominated by the background flow velocity $u_{E\times B}$ [38]. The dominance of the $E\times B$ flow in the SOL has been shown by a comparison of reflectometry with direct measurements of the plasma potential using a ball pen probe in ASDEX Upgrade [39, 40].

Figure 7 reveals a high velocity of about 4 km/s into the electron-diamagnetic drift direction for the confined plasma. Across the separatrix and in the near SOL, the velocity decreases. A radial shift of 5 mm is found between the velocity reversals from Doppler reflectometry and probe data. The transition from the electron to the ion-diamagnetic drift direction is generally expected to occur at the separatrix. This might be the case for the smooth transition of the Doppler reflectometry profile considering the radial uncertainty of the separatrix position of ± 5 mm. The Langmuir probes in contrast, indicate an abrupt reversal of $u_\perp$ at about 1 cm outside the separatrix. This strong shear layer was reproduced by correlating different probe tips during different strokes in several discharges and in different plasma conditions (lower density Ohmic, L- and H-mode). The result remains qualitatively the same.

A similar abrupt reversal of $u_\perp$ has also been observed by probes in the low temperature plasma of the TJ-K stellarator [22]. In the Alcator C-Mod tokamak two discrete poloidal velocities were observed with a crossover just outside the separatrix [41]. The latter results were based on linear fits to wavenumber-frequency spectra obtained from a gas puff imaging diagnostics. The lack of intermediate velocities around zero is consistent to the present probe results, but differs from earlier probe measurements in Alcator C-Mod [42].

The shear layer is now characterized in more detail. To this end, figure 8 shows cross-correlation functions of the signals from probe tips number 8 and 9 based on 2 ms time windows around the flow reversal at $d_s \approx 10$ mm. At $d_s = 7$ mm (figure 8a), the correlation maximum is reached at $\tau \approx 4\,\mu$s. This corresponds to a propagation velocity of ≈ 1.4 km/s into the electron-diamagnetic drift direction. Further outside, at $d_s = 12$ mm (figure 8c), maximum correlation is reached at $\tau \approx -3\,\mu$s and the propagation velocity points into the ion-diamagnetic drift direction. Not only the peak position, but if mirrored at $\tau = 0\,\mu$s, also the asymmetric shape of the cross-correlation functions at $d_s = 7$ and 12 mm are similar. Auto-correlation functions are always symmetric around the maximum correlation of 100 % at $\tau = 0$. Cross-correlation functions are asymmetric, if the signals are asymmetric in time and the shape of the dominant structure changes between both observations. Thus, the asymmetric shapes in figure 8 indicate that blobs are not only asymmetric in time, as reported from several machines [43], but also that their shape changes significantly within $3\,\mu$s.

At some position in between the opposed perpendicular velocities, a point with a mean velocity of zero should be present. The cross-correlation function at this point

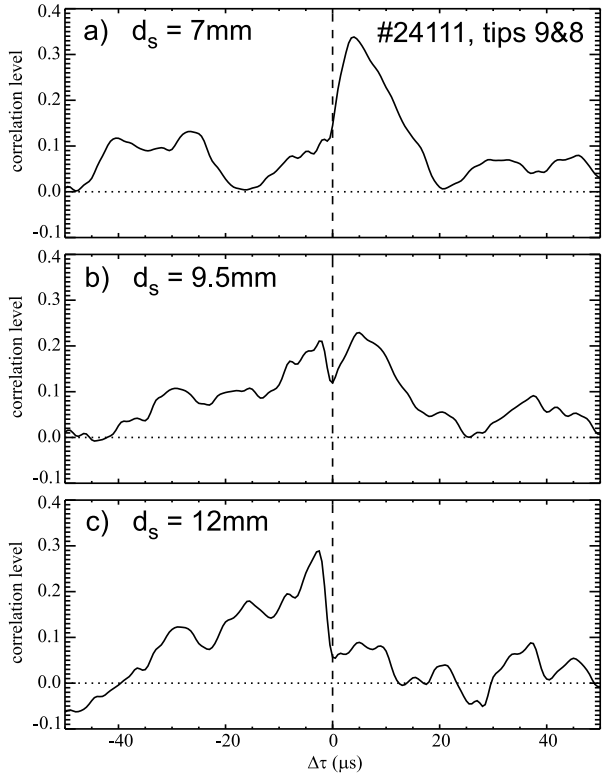

Figure 8. Cross-correlation functions of the ion-saturation-current fluctuations measured with two poloidally separated Langmuir probes at different distances to the separatrix d_s in ASDEX Upgrade.

would be expected to be centrally peaked at $\tau = 0\,\mu$s with a low peak correlation level, due to a dominant radial propagation at this position. Figure 8b shows the correlation function at $d_s = 9.5\,$mm. The correlation level is indeed lower, but the correlation function exhibits two peaks at $\tau \neq 0\,\mu$s instead of a single one at $0\,\mu$s. The two correlation maxima are found at similar τ values as the single peaks at the neighboring radial positions. This indicates that the fluctuations at $d_s = 9.5\,$mm are dominated by the structures propagating at a distance into opposite directions.

From the auto-correlation time measured with single probes of $\tau_{auto} \approx 6\,\mu$s and a propagation velocity of $|v_\perp| \approx 1.4\,$km/s on both sides of the shear layer, it is possible to estimate the auto-correlation length $L_{corr} = \tau_{auto}\,|v_\perp| \approx 8 \pm 2\,$mm. This is also the characteristic scale the Doppler reflectometer is most sensitive to. Interestingly, L_{corr} is constant across the shear layer and also the statistical moments in figure 5 seem not to be affected by the abrupt $u_\perp$ reversal. Hence, there are no clear indications for the decorrelation of dominant fluctuations by the shear flow.

6. Conclusions

Plasma turbulence was investigated experimentally using Langmuir probes in the edge region of Ohmic discharges in the ASDEX Upgrade tokamak. The electron density

and temperature profiles from probe measurements show reasonable agreement with results from lithium beam, Thomson scattering and ECE diagnostics. Furthermore, the propagation velocity of the turbulent structures perpendicular to the magnetic field, which is close to a poloidal velocity, was deduced from cross-correlation analysis between separated probes. The results fit well to the velocity profile deduced from Doppler reflectometry, which was pointed out to be dominated by the $E \times B$ flow velocity imposed by the radial electric field [38]. Radially resolved PDFs of ion-saturation current fluctuations have been analyzed. A parabolic relation between skewness and kurtosis of the PDFs has been found similar to observations in other devices [36]. Intermittent structures were observed with negative amplitudes (*holes*) in the confined plasma and positive amplitudes (*blobs*) in the SOL. Holes and blobs appear radially separated. They seem to be born in a common process at the nominal separatrix position, which is known with an accuracy of ± 5 mm. This is consistent with findings from DIII-D [6] and shows that blobs are not the foothills of avalanches launched in the plasma core.

An abrupt reversal of the poloidal propagation velocity of the fluctuations was found in the SOL at a distance of about 1 cm from the nominal separatrix position. This shear layer seems to have little influence on the correlation length of the turbulent structures nor on the fluctuation level. The radial shift between the nominal separatrix position and the shear layer is surprising and might be explained by the uncertainties in probe and separatrix positions. In case that the real separatrix coincides with the shear layer, the intermittent structures would be born just inside the separatrix, but the blobs are not created right at the shear layer.

Acknowledgments

The authors thank A. Kirk, F. Ryther and M. Maraschek for support and BN would like to acknowledge valuable discussions with G. Antar.

References

[1] S. Zweben and R. Gould, Nucl. Fusion **25**, 2, 171 (1985).
[2] M. Endler *et al.*, Nucl. Fusion **35**, 11, 1307 (1995).
[3] R. Moyer *et al.*, Plasma Phys. Controll. Fusion **38**, 8, 1273 (1996).
[4] M. Pedrosa *et al.*, Phys. Rev. Lett. **82**, 18, 3621 (1999).
[5] E. Sanchez *et al.*, Phys. Plasmas **7**, 5, 1408 (2000).
[6] J. Boedo *et al.*, Phys. Plasmas **10**, 5, 1670 (2003).
[7] J. Alonso *et al.*, Plasma Phys. Controll. Fusion **48**, 12B, B465 (2006).
[8] M. Agostini *et al.*, Phys. Plasmas **14**, (2007).
[9] S. Zweben *et al.*, Plasma Phys. Controll. Fusion **49**, 7, S1 (2007).
[10] G. Y. Antar *et al.*, Phys. Plasmas **10**, 2, 419 (2003).
[11] G. Antar, M. Tsalas, E. Wolfrum, and V. Rohde, Plasma Phys. Controll. Fusion **50**, 9, (2008).
[12] T. Carter, Phys. Plasmas **13**, 1, (2006).
[13] T. Windisch, O. Grulke, and T. Klinger, Phys. Plasmas **13**, 12, (2006).
[14] G. Antar, J. Yu, and G. Tynan, Phys. Plasmas **14**, 2, (2007).
[15] I. Furno *et al.*, Phys. Plasmas **15**, 5, (2008).

[16] A. Diallo *et al.*, Phys. Rev. Lett. **101**, 11, (2008).
[17] S. I. Krasheninnikov, D. A. D'Ippolito, and J. R. Myra, J. Plasma Phys. **74**, (2008).
[18] D. Russell *et al.*, Phys. Rev. Lett. **93**, 26, (2004).
[19] N. Bisai *et al.*, Phys. Plasmas **12**, 10, (2005).
[20] O. E. Garcia *et al.*, Plasma Phys. Controll. Fusion **48**, 1, L1 (2006).
[21] W. Fundamenski *et al.*, Nucl. Fusion **47**, 5, 417 (2007).
[22] T. Happel *et al.*, Phys. Rev. Lett. **102**, 25, (2009).
[23] J. Myra *et al.*, Phys. Plasmas **13**, 9, (2006).
[24] A. Herrmann and O. Gruber, Fusion Sci. Technol. **44**, 3, 569 (2003).
[25] M. Reich *et al.*, Plasma Phys. Controll. Fusion **46**, 5, 797 (2004).
[26] R. Fischer, E. Wolfrum, and J. Schweinzer, Plasma Phys. Controll. Fusion **50**, 8, (2008).
[27] N. Salmon, Int. J. Infrared Millim. Waves **15**, 1, 53 (1994).
[28] B. Kurzan, M. Jakobi, and H. Murmann, Plasma Phys. Controll. Fusion **46**, 1, 299 (2004).
[29] D. L. Rudakov *et al.*, Rev. Sci. Instrum. **75**, 10, 4334 (2004).
[30] G. Antar *et al.*, Phys. Rev. Lett. **87**, 6, (2001).
[31] C. Hidalgo, B. van Milligen, and M. Pedrosa, C. R. Physique **7**, 6, 679 (2006).
[32] Y. Xu, S. Jachmich, and R. Weynants, Plasma Phys. Controll. Fusion **47**, 10, 1841 (2005).
[33] G. Xu *et al.*, Nucl. Fusion **49**, 9, (2009).
[34] J. Boedo *et al.*, Phys. Plasmas **8**, 11, 4826 (2001).
[35] S. Zweben *et al.*, Nucl. Fusion **44**, 1, 134 (2004).
[36] B. Labit *et al.*, Plasma Phys. Controll. Fusion **49**, 12B, B281 (2007).
[37] F. Sattin *et al.*, Plasma Phys. Controll. Fusion **51**, 5, (2009).
[38] G. D. Conway *et al.*, Nucl. Fusion **46**, 9, S799 (2006).
[39] J. Adamek *et al.*, J. Nucl. Mater. 390-391, 1114 (2009).
[40] J. Adamek *et al.*, (to be submitted).
[41] I. Cziegler, J. Terry, and B. LaBombard, Bull. Am. Phys. Soc. **52**, 11, (2007).
[42] B. LaBombard, S. Gangadhara, B. Lipschultz, and C. S. Pitcher, J. Nucl. Mater. **313**, 995 (2003).
[43] G. Antar, Contrib. Plasma Phys. **44**, 1-3, 217 (2004).